ELSEVIER

www.elsevier.nl/locate/carres

Carbohydrate Research 322 (1999) 77–86

CARBOHYDRATE RESEARCH

Disaccharide conformational maps: how adiabatic is an adiabatic map?

Carlos A. Stortz *,[1]

Departamento de Química Orgánica-CIHIDECAR, Facultad de Ciencias Exactas y Naturales, UBA, Ciudad Universitaria, 1428 Buenos Aires, Argentina

Received 9 April 1999; accepted 9 July 1999

Abstract

The 'adiabatic' (ϕ, ψ) potential-energy surface of the disaccharide α-D-galactopyranosyl-(1→3)-β-D-galactopyranose was obtained by several established methods, using the MM3 molecular mechanics force field. The constrained minimizations throughout the whole grid were carried out using sharply different dielectric constants. The attainment of the 'true' adiabatic map is very difficult due to the 'multiple minimum problem', originating in the large number of exocyclic pendant groups present in a disaccharide. However, these results suggest that at low dielectric constants, the usual approach starting with conformers carrying cooperative hydrogen bonds results in a good approximation to the true adiabatic map, while at high dielectric constants this approach fails due to the damping of electrostatic and hydrogen-bonding interactions.

Keywords: Conformational analysis; Disaccharide maps; MM3; Adiabatic maps

1. Introduction

Conformational analysis of disaccharides is usually accompanied by the generation of a Ramachandran-like conformational map as a tool in understanding oligosaccharide conformational structures [1–3]. In these maps the energy is determined for all mutual orientations of the two monosaccharide residues, expressed by the glycosidic angles ϕ and ψ. First studies were carried out by rigid residue analysis [3]. However, by allowing all variables to relax, Melberg and Rasmussen [4–6] initiated flexible residue analysis by 1979. These studies were extended in the late 1980s [7–12], giving rise to the first fully relaxed energy maps of many disaccharides. When generating these Ramachandran maps, it should be borne in mind that the actual conformational hypersurface of a disaccharide carries, for each ϕ, ψ combination, the influence of the orientations of secondary hydroxyl groups, hydroxymethyl groups and the primary hydroxyl groups, all of which may affect the calculated final energy by several kilocalories (the 'multiple minimum problem' [1–3]). For a disaccharide formed by two hexopyranose residues and considering the three staggered positions for the ten exocyclic groups, 59,049 (3^{10}) different starting points are possible for the construction of the map [3,13,14]. Thus, different starting points will yield different minima after geometry optimization.

An 'adiabatic' map is generated by plotting the lower-energy values found at each grid

* Fax: +54-11-4576-3346.

E-mail address: stortz@qo.fcen.uba.ar (C.A. Stortz)

[1] Research Member of the National Research Council of Argentina (CONICET).

0008-6215/99/$ - see front matter
PII: S0008-6215(99)00207-4

point [15]. The outcome is that, at least theoretically, the true adiabatic map for a disaccharide can only be obtained after calculating 59,049 relaxed maps and determining, for each ϕ/ψ combination, the one with the lowest energy. Even with present resources, and using a fast molecular mechanics method, this task is very difficult (one adiabatic map in a $20 \times 20°$ grid would take more than three years in a single CPU for minimizations taking an average of 5 s each). This problem has been extensively recognized since the early flexible residue analyses [4–6,10–15]. However, it was found that the hydroxymethyl groups in monosaccharides show a marked trend to stay at preferential positions (usually *gg* and *gt*) [11,14]. Furthermore, it was determined that the secondary hydroxyl groups are likely to form a 'crown' of cooperative hydrogen bonds, oriented either clockwise (c) or reverse clockwise (r) around the pyranose ring [9]. In this way, each monosaccharidic unit was considered [15,16] only in the *gt*r, *gt*c, *gg*c and *gg*r conformations, thus leading to only 16 starting points for the disaccharide. This approach has been extensively used, among others, by Dowd et al. [16–19], who studied different disaccharides using MM3. Sometimes the starting conformers were not just 16, but 24 when a different arrangement of hydroxyl groups was added [17,18], 36 when the hydroxymethyl groups were considered at the three available positions [20,21] or some other figures [22]. The same approach was even adopted to emulate aqueous solutions [23,24], where such circuits of hydrogen bonds might not form at all. The multiple minimum problem was also tackled with less systematic procedures, such as iterative manual searches [11,15,25–27]. Tvaroška and co-workers tried to overcome this problem with the program RAMM, which finds the energetically most favorable combinations of the pendant group orientations for each ϕ,ψ pair, using a random sampling technique [13,22,28]. Another way to elude the multiple minimum problem is to explore the conformational space of disaccharides by molecular dynamics (MD) simulations [22,29,30], an expanding methodology. These simulations were also combined with Monte Carlo techniques in order to increase their efficiency to cross energy barriers [31,32].

French and co-workers [14,16] have pointed out the problems arising from minimization with the MM2 'standard driver', for which the inelastic deformations are transmitted to the next structure, and thus suggested the use of a driver in which each point of each relaxed surface is generated directly from the same starting point, in order to avoid these propagations of deformations.

Herein is presented the mapping of the disaccharide α-D-Gal*p*-(1→3)-β-D-Gal*p* (**1**) [25–27] using MM3 [33] at either $\varepsilon = 3$ or $\varepsilon = 80$. The influence of using either driver systematically, and of an iterative manual searching procedure, on the adiabaticity of the final maps is discussed.

2. Methods

Calculations were carried out on a Sun SparcStation 10 computer, using the molecular mechanics program MM3 (92) (QCPE, Indiana University, USA), developed by Allinger and co-workers [33]. The MM3 routines were modified as suggested [34] by changing the maximum atomic movement from 0.25 to 0.10 Å. Minimization (by the block diagonal Newton–Raphson procedure for grid points, using the full-matrix procedure for the minima) was terminated when the average movement converged to a value lower than 10^{-4} Å. The dihedrals ϕ and ψ (also called ϕ_H and ψ_H) are defined by atoms H-1′–C-1′–O-3–C-3 and H-3–C-3–O-3–C-1′, respectively, with the usual sign conventions [27]. NOE theoretical calculations and average linkage rotations were calculated as reported elsewhere [25,27].

Sixteen starting conformers of the disaccharide were generated by minimization of structures with the adequate geometry: their glycosidic torsional angles were around ϕ, ψ $-40°, -40°$ (minimum **B**) [27], their monosaccharide constituents were $^4C_1$ ring conformers with either *gt* ($\theta_{O\text{-}5\text{–}C\text{-}5\text{–}C\text{-}6\text{–}O\text{-}6} \approx 60°$) or *gg* ($\theta_{O\text{-}5\text{–}C\text{-}5\text{–}C\text{-}6\text{–}O\text{-}6} \approx -60°$) orientation of the hydroxymethyl groups. As suggested [9], clockwise (c) or reverse clockwise (r) ori-

Table 1
Approx. starting angles (°) for the c and r torsional orientations of the hydroxyl groups of **1**

Torsional angle	α-Non-reducing unit		β-Reducing unit	
	c	r	c	r
H-1–C-1–O-1–H(O-1)			−60	60
H-2–C-2–O-2–H(O-2)	60	180	60	−60
H-3–C-3–O-3–H(O-3)	180	60		
H-4–C-4–O-4–H(O-4)	60	60	−60	60
C-5–C-6–O-6–H(O-6)	−60 (*gt*)	−60	−60 (*gt*)	−60
	60 (*gg*)		60 (*gg*)	

entations were chosen for the secondary hydroxyl groups. The primary hydroxyl groups were also settled in a position that may give hydrogen-bonding possibilities (Table 1). As the conformation of each ring is, a priori independent from that of the other, four orientations of hydroxyl groups and four of hydroxymethyl groups are possible, thus leading to the 16 starting conformations.

Each starting conformer led to a different ϕ/ψ relaxed map. Using both dihedral drivers (see below), ϕ and ψ were fully varied (through the whole −180 to 180° grid) using a 20° grid step. At each point, energies were calculated after minimization with restraints for these two angles but allowing the other variables to relax. Both $\varepsilon = 3$ and $\varepsilon = 80$ were applied, using either MM3 Driver 2, which at each point takes the previously calculated grid point as the starting point for calculations, or MM3 Driver 4, which always uses the same starting conformer to calculate all grid points directly (Fig. 1). 'Adiabatic' maps [15] were constructed in each case using, for each grid point, the lowest-energy value for each set of 16 relaxed maps. The contribution of each relaxed map to the 'adiabatic' map was evaluated from their probability distributions assuming no entropy differences:

$$P_i = \frac{\sum_{\phi\psi} \exp(-E_{\phi\psi}/RT)}{\sum_i \sum_{\phi\psi} \exp(-E_{\phi\psi}/RT)}$$

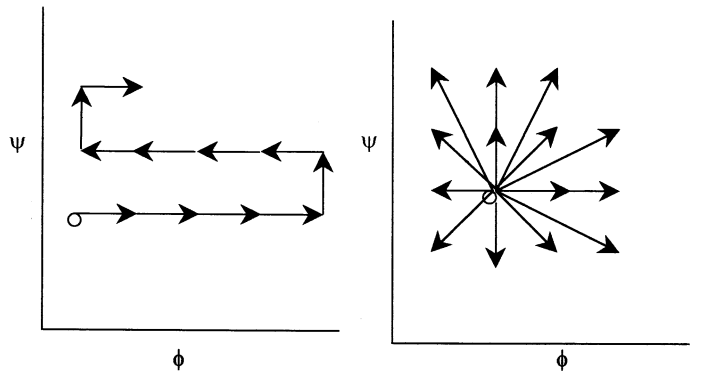

Driver 2

ϕ,ψ= –40,–40 →
–20, –40 →
0, –40 →
……..
–60,–40 →
–40,–40 →
–40,–20 →
–60,–20 →
–80,–20 →
……..
0,20 →
……..
–40,180 →
–40,160 →
……..
–40,0→
……..
–40,–40

Driver 4

–40,–40 → –20, –40
–40,–40 → 0, –40
……..
–40,–40 → –60,–40
–40,–40 → –60,–20
–40,–40 → –80,–20
……..
–40,–40 → –40, –20
–40,–40 → –40, 0
……..
–40,–40 → 0,20
……..
–40,–40 → –40,180
–40,–40 → –40,160
……..
–40,–40 → –60,–60

Fig. 1. Operating scheme of MM3 Drivers 2 and 4.

In a different procedure, another 'adiabatic' map was generated following an iterative procedure reported elsewhere [15,25–27]. Briefly, some different starting geometries were chosen, using the lower-energy conformations for α- and β-D-galactose [35] and checking the effects of rotations of alternate pairs of hydroxymethyl and hydroxyl groups. To identify the lowest energy on each ϕ, ψ grid point, many starting conformations were minimized. The generated points served as starting points for the next ones, radially from each starting point, in an iterative manner. As it was pointed out [15], the amount of additional searching done for each point was arbitrary, and therefore cannot be automated.

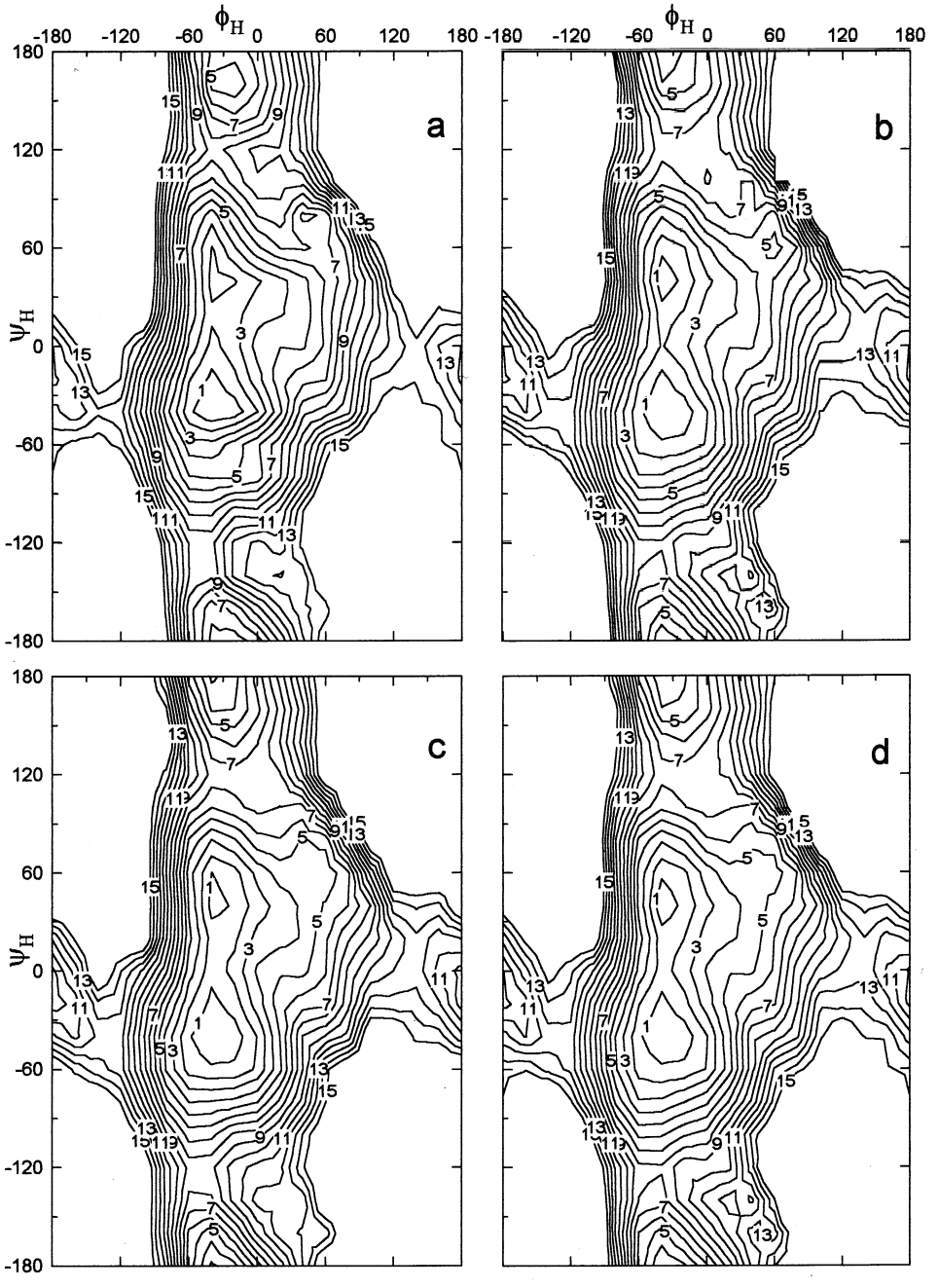

Fig. 2. 'Adiabatic' maps obtained for compound **1** using MM3 ($\varepsilon = 3$) with (a) Driver 2, (b) Driver 4, (c) an iterative method (see Section 2). (d) 'True' adiabatic map. Isoenergy contour lines are graduated in 1 kcal mol^{-1} increments above the global minimum.

3. Results and discussion

The MM3-generated conformational maps of the disaccharide α-D-Gal*p*-(1→3)-β-D-Gal*p* (**1**) at a dielectric constant 3.0 were obtained both using the MM3 dihedral drivers 2 and 4 (Fig. 1), starting from 16 different initial conformers. The maps with the lowest-energy values for each grid point are shown in Fig. 2(a) for dihedral driver 2 and Fig. 2(b) for dihedral driver 4. Fig. 2(c) shows the map obtained with an iterative method (see Section 2). With those three 'adiabatic' maps, a more representative 'true' adiabatic map was constructed (Fig. 2(d)), in which each grid point takes the lower value. Fig. 3 displays the energy differences between the 'adiabatic' map obtained by each method and the 'true' adiabatic map. As shown, none of the three methods produced the lower-energy points for the whole grid, as it was already suggested [3]. The work performed with Driver 4 yielded lower-energy values than that carried out with Driver 2. The latter gave rise to many high-energy values (some more than 3 kcal mol^{-1} above those obtained by other methods), especially for the strip with $\psi = -60°$, close to the termination of the cycle, where inelastic deformations [14] led to high-energy values for the 16 starting conformers. Table 2 indicates the contributions of each of the three methods to the 'true' adiabatic map. As shown, using Driver 2, more than half of the grid points have energies with an average of 2.1 kcal mol^{-1} above their minimum values. Most of the 16 starting conformations yielded points that were used to construct the maps, but more than two-thirds of their population arises from conformers with the β-D-galactose unit in *gt* orientation. Also, starting conformers with alternate configurations of secondary hydroxyl groups (rc and cr) double the population of those with the same configuration (cc

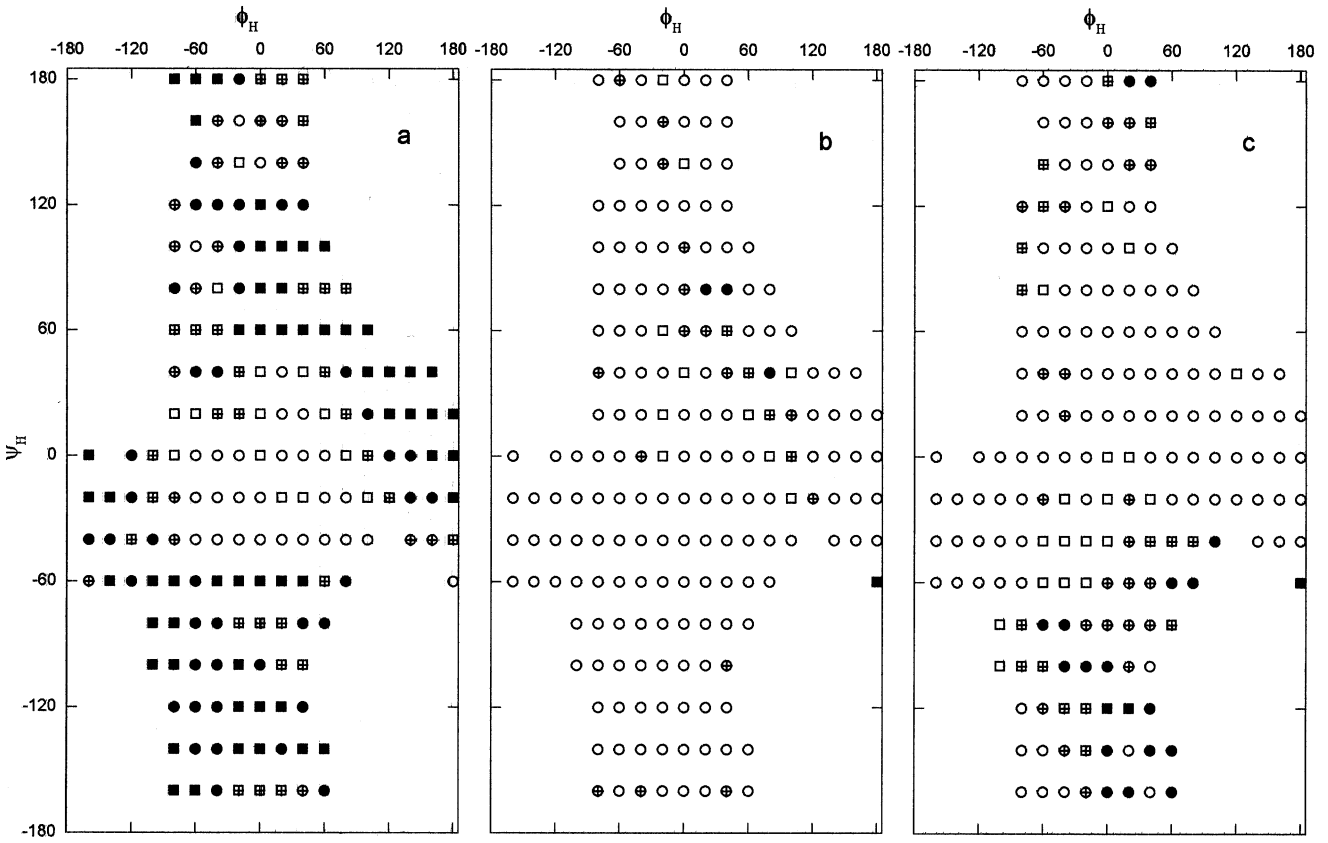

Fig. 3. Plot of the excess energies of the grid points from each 'adiabatic' map to those of the 'true' adiabatic map ($\varepsilon = 3$). 'Adiabatic' maps were obtained with: (a) Driver 2, (b) Driver 4, (c) an iterative method (see Section 2). Excess energies are indicated as follows: (○) 0–0.1 kcal; (□) 0.1–0.3 kcal; (⊕) 0.3–0.6 kcal; (⊞) 0.6–1 kcal; (●) 1–2 kcal; (■) >2 kcal mol^{-1}.

Table 2
Contribution to the MM3-generated 'true' adiabatic map of **1** at $\varepsilon = 3.0$ by each method

Limit value (kcal mol^{-1})	Percentage of grid [a] below limit			Average excess (kcal mol^{-1})		
	Driver 2	Driver 4	Iterative	Driver 2	Driver 4	Iterative
0.1	14	81	59	1.5	0.5	0.7
0.5	29	94	77	1.7	1.0	1.1
1.0	48	98	89	2.1	1.7	1.5

[a] Percentage of the 186 grid points within a 15 kcal mol^{-1} low-energy window that have an energy equal to or less that of the 'true' adiabatic map plus the limit value.

and rr). The actual minimum-energy starting point corresponds to a *gggt*cr orientation. Table 3 shows the values of its exocyclic angles.

The same procedures were repeated with $\varepsilon = 80$. Fig. 4 shows the three resulting maps, Fig. 5 shows the energy differences of each map from the 'true' adiabatic map (Fig. 4(c)), and Table 4 indicates their contributions to this true adiabatic map. In this instance, the iterative search procedure by itself yielded the true adiabatic map (Figs. 4(c) and 5, Table 4). Drivers 2 and 4 gave rise to a map with energies averaging 0.6 and 0.9 kcal mol^{-1} above the adiabatic map, respectively. Even considering points with 0.5 kcal mol^{-1} difference, Driver 4 failed to find true minima on 81% of the grid. As expected, the deficiency of the systematic methods at this dielectric constant arises from the fact that none of the initial 16 starting conformers has the lower-energy conformation of the exocyclic groups. This is obvious when using a method where the electrostatic contributions were intentionally damped [2,22,25] by using a dielectric constant of 80, for which hydrogen bonding has almost no effect, and thus the r and c circuits are meaningless. The geometry of the actual global minimum (found by the iterative search procedure) is shown in Table 3. In this conformer, both monosaccharide units had hydroxymethyl groups in *gt* orientation, the unit of β-galactose had their secondary hydroxyl groups in an r arrangement, but the α-galactose unit has no recognizable pattern (Table 3).

Table 3
Exocyclic angles (°) for the minimum-energy conformations encountered for compound **1** in the region $\phi, \psi \approx -40°, -40°$ at $\varepsilon = 3$ and $\varepsilon = 80$

Torsional angle	$\varepsilon = 3$ [a]	$\varepsilon = 80$ [b]
α-D-Galactose unit		
H-1′–C-1′–O-1′–C-3 = ϕ	−39	−40
H-2′–C-2′–O-2′–H(O-2′)	66	53
H-3′–C-3′–O-3′–H(O-3′)	−159	−44
H-4′–C-4′–O-4′–H(O-4′)	−68	52
O-5′–C-5′–C-6′–O-6′	−64	70
C-5′–C-6′–O-6′–H(O-6′)	71	180
β-D-Galactose unit		
H-1–C-1–O-1–H(O-1)	63	47
H-2–C-2–O-2–H(O-2)	−54	−50
H-3–C-3–O-3–C-1′ = ψ	−39	−39
H-4–C-4–O-4–H(O-4)	64	60
O-5–C-5–C-6–O-6	68	70
C-5–C-6–O-6–H(O-6)	−65	180

[a] Corresponds to a *gggt*cr orientation.
[b] Corresponds to a *gt*r orientation of the β-Gal unit, and no recognizable pattern at the secondary hydroxyl groups of the α-Gal unit.

Contrasting the maps generated at a low dielectric constant, here the lower-energy points (within a 15 kcal mol^{-1} low-energy window) arise from a few starting conformers. More than 80% of the population of the Driver 4 map arises from starting conformers in which both hydroxymethyl groups carry *gt* orientation (mainly *gtgt*rr), while less than 1% arises from both monosaccharidic units with *gg* orientation. No major effect of the secondary hydroxyl group arrangements was found, although those starting with r orientation yielded a higher population on the adiabatic map than those with c orientation.

According to literature [23,35], the hydroxymethyl groups of galactose are oriented *gt* or *tg* rather than *gg*. However, in this calculation *gt* and *gg* orientations were used, because it was found that *tg* orientation gives abnormally high energy values in molecular mechanics calculations [35].

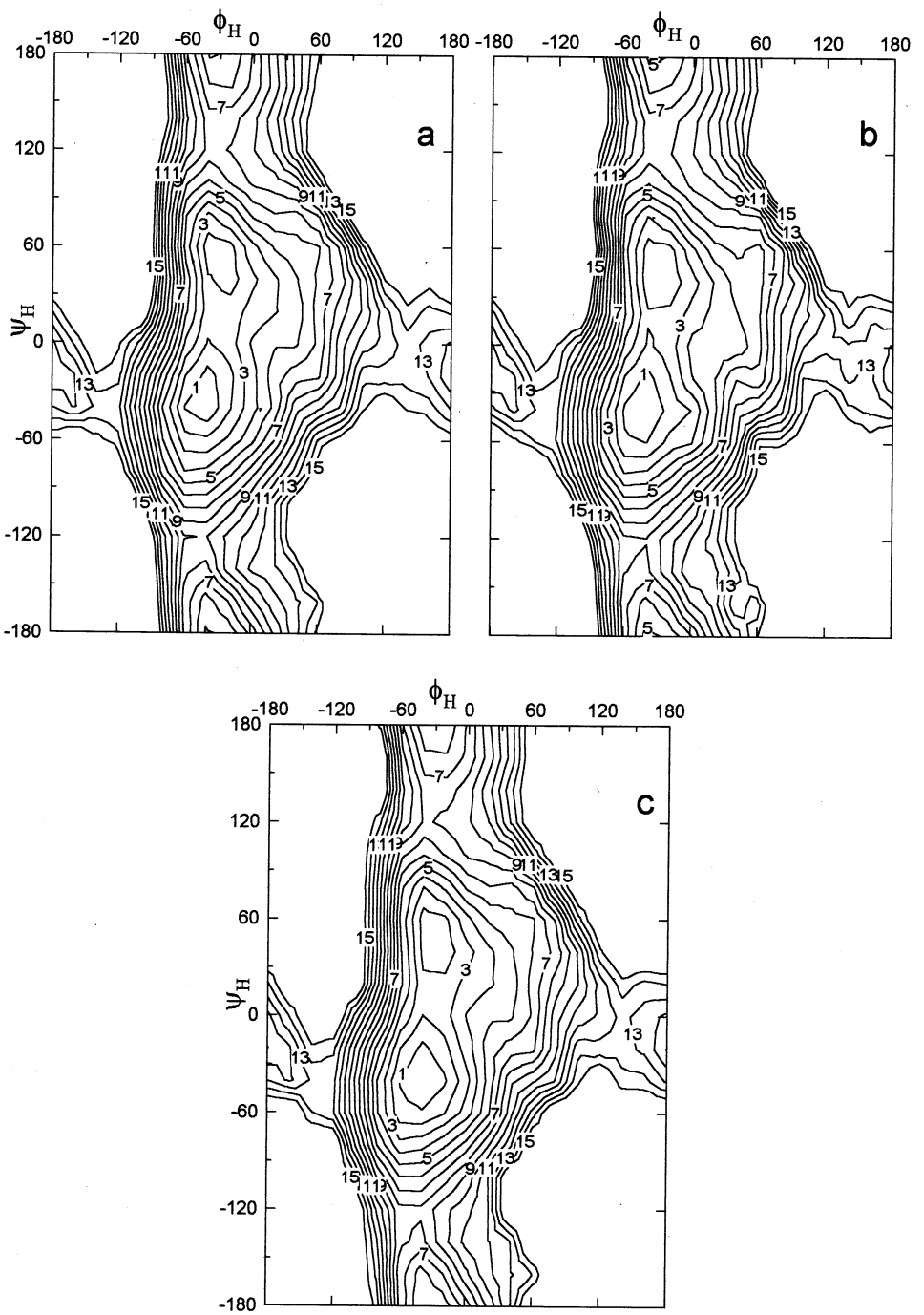

Fig. 4. 'Adiabatic' maps obtained for compound **1** using MM3 ($\varepsilon = 80$) with (a) Driver 2, (b) Driver 4, (c) an iterative method (see Section 2). Isoenergy contour lines are graduated in 1 kcal mol^{-1} increments above the global minimum.

Table 5 shows the average NOE and linkage rotations predicted from the adiabatic maps at both dielectric constants. Their comparison with experimental values indicates a better agreement with the calculations carried out at $\varepsilon = 80$.

The need for reliable methods for generating disaccharide 'adiabatic' maps was recognized at an earlier time [1] and discussed extensively [3,11,13–15]. French and co-workers have suggested the use of the so-called 'new driver' [14,16] (later brought into MM3

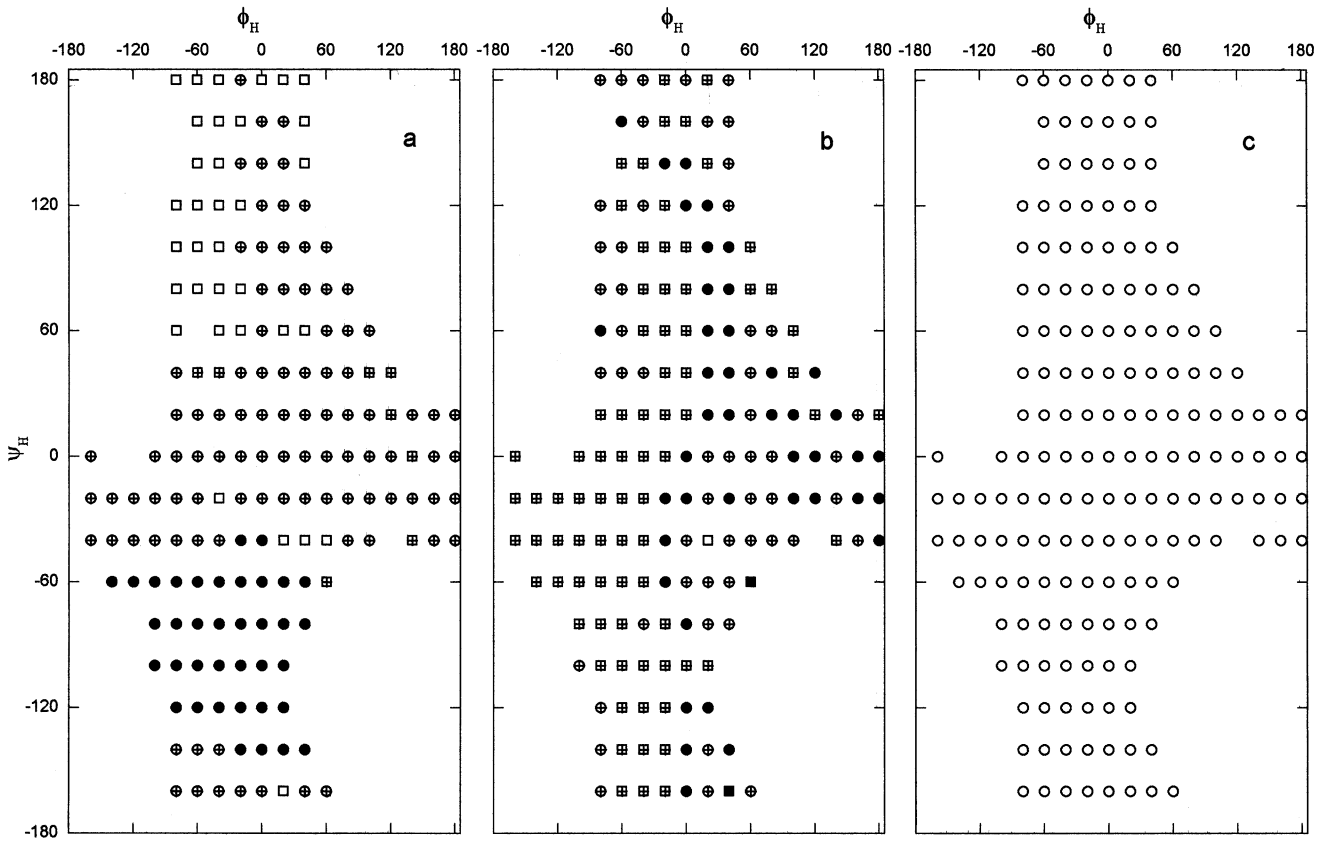

Fig. 5. Plot of the excess energies of the grid points from each 'adiabatic' map to those of the 'true' adiabatic map ($\varepsilon = 80$). 'Adiabatic' maps were obtained with: (a) Driver 2, (b) Driver 4, (c) an iterative method (see Section 2). Excess energies are indicated as follows: (○) 0–0.1 kcal; (□) 0.1–0.3 kcal; (⊕) 0.3–0.6 kcal; (⊞) 0.6–1 kcal; (●) 1–2 kcal; (■) >2 kcal mol^{-1}.

Table 4
Contribution to the MM3-generated 'true' adiabatic map of **1** at $\varepsilon = 80.0$ by each method

Limit value (kcal mol^{-1})	Percentage of grid [a] below limit			Average excess (kcal mol^{-1})		
	Driver 2	Driver 4	Iterative	Driver 2	Driver 4	Iterative
0.1	0	0	100	0.6	0.9	
0.5	61	19	100	1.0	1.0	
1.0	79	75	100	1.3	1.4	

[a] Percentage of the 176 grid points within a 15 kcal mol^{-1} low-energy window that have an energy equal to or less that of the 'true' adiabatic map plus the limit value.

Table 5
Experimental and calculated NOE values and linkage rotations for the disaccharide α-D-Gal*p*-(1→3)-β-D-Gal*p*

	NOE on H-3 [a]	NOE on H-4 [a]	Linkage rotation (Λ, in °)
MM3, $\varepsilon = 3$	0.41	0.29	−10
MM3, $\varepsilon = 80$	0.31	0.47	+22
Experimental [25,36]	0.32	0.53	+13

[a] When irradiating H-1′, relative to the NOE on H-2′.

as Driver 4) in the hope of arriving at better results, together with a combination of low-energy starting points based on their hydrogen-bonding abilities [9]. The same group has successfully applied the method to the MM3 analysis of many disaccharides [16–19] at dielectric constants close to four.

In more recent papers [23,24,37], the method was extended to simulations of water behavior by using a dielectric constant close to 80. For ionic solutions this value is higher than that of the water in the first solvation shell, where it can reach values as low [38] as six. The effect of using a constant close to 80 is equivalent to neglecting electrostatic and hydrogen-bonding interactions [22,25]. However, it has been used in order to obtain better agreement with experimental values in aqueous solutions [39], as in this work (Table 5). This paper shows that, at least with the disaccharide under study, high-dielectric-constant MM3 calculations with Driver 4 exhibit large failures to produce an adiabatic map. Furthermore, Driver 2 gives rise to a far better map, which can even be improved if this option is also used backwards (i.e. from $\psi = -40°$ to lower values). In this way, the large errors appearing in the regions with $\psi = -60$ to $-140°$ (Fig. 5), where the inelastic deformations appearing in the long way that leads to them, generating high energy values, are avoided. Actually, the 'true' adiabatic map was obtained in the present work by a non-systematic, iterative procedure that has encountered a better approach to the true surface.

As it has been pointed out, without a full conformational search of the 59,049 starting conformers, no true adiabatic map can be produced [3,10,14,15]. However, it is possible to reach near adiabaticity, by a combination of the three methods shown previously. Certainly, it is impossible to automate the iterative method, which means consuming considerable CPU time, as well as making a sizeable demand on the efforts of an experienced researcher. However, reports of adiabatic maps with high dielectric constants and starting conformers with the classical clockwise–anticlockwise orientation of the secondary hydroxyl groups should be treated with due care.

There are alternative approaches for the creation of a potential-energy surface, like the use of random sampling techniques [22] such as RAMM [13,28], the use of heuristic procedures like CICADA [40,41] or applications of simulations based on molecular dynamics [22,29,30], Monte Carlo [42], or combinations of both [31,32]. Even when the construction of an adiabatic map is not attempted [43], the generation of the local minima is usually required. The results shown in this paper indicate that the determination of the local minima from the combination of a small number of relaxed maps may fail, and it indeed does, at high dielectric constants. Although the conformational maps obtained by each method are roughly similar (Figs. 2 and 4), the fact that many properties of carbohydrates depend strongly on small differences in energy leads to a struggle for the greatest possible accuracy [3] on the actual adiabatic character of the generated maps.

Acknowledgements

This work was supported by a grant from UBA (TX-014). Helpful discussions with Drs A.S. Cerezo, R. Erra-Balsells and M.S. Maier are also acknowledged.

References

[1] A.D. French, J.W. Brady, *ACS Symp. Ser.*, 430 (1990) 1–19.
[2] S.B. Engelsen, K. Rasmussen, *Int. J. Biol. Macromol.*, 15 (1993) 56–62.
[3] A.D. French, M.K. Dowd, *J. Mol. Struct.* (*Theochem*), 286 (1993) 183–201.
[4] S. Melberg, K. Rasmussen, *Carbohydr. Res.*, 69 (1979) 27–38.
[5] S. Melberg, K. Rasmussen, *Carbohydr. Res.*, 71 (1979) 25–34.
[6] S. Melberg, K. Rasmussen, *Carbohydr. Res.*, 78 (1980) 215–224.
[7] I. Tvaroška, S. Pérez, *Carbohydr. Res.*, 149 (1986) 389–410.
[8] A.D. French, *Biopolymers*, 27 (1988) 1519–1523.
[9] S.N. Ha, L.J. Madsen, J.W. Brady, *Biopolymers*, 27 (1988) 1927–1952.
[10] A.D. French, *Carbohydr. Res.*, 188 (1989) 206–211.
[11] V. Tran, A. Buléon, A. Imberty, S. Pérez, *Biopolymers*, 28 (1989) 679–690.
[12] A. Imberty, V. Tran, S. Pérez, *J. Comput. Chem.*, 11 (1989) 205–216.

[13] I. Tvaroška, T. Kozár, M. Hricovíni, *ACS Symp. Ser.*, 430 (1990) 162–176.
[14] A.D. French, V.H. Tran, S. Pérez, *ACS Symp. Ser.*, 430 (1990) 191–212.
[15] V.H. Tran, J.W. Brady, *Biopolymers*, 29 (1990) 961–976.
[16] M.K. Dowd, P.J. Reilly, A.D. French, *J. Comput. Chem.*, 13 (1992) 102–114.
[17] M.K. Dowd, J. Zeng, A.D. French, P.J. Reilly, *Carbohydr. Res.*, 230 (1992) 223–244.
[18] M.K. Dowd, A.D. French, P.J. Reilly, *Carbohydr. Res.*, 233 (1992) 15–34.
[19] M.K. Dowd, A.D. French, P.J. Reilly, *J. Carbohydr. Chem.*, 14 (1995) 589–600.
[20] S.B. Engelsen, S. Pérez, I. Braccini, C. Hervé du Penhoat, *J. Comput. Chem.*, 16 (1995) 1096–1119.
[21] S.B. Engelsen, K. Rasmussen, *J. Carbohydr. Chem.*, 16 (1997) 773–788.
[22] C.W. von der Lieth, T. Kozár, W.E. Hull, *J. Mol. Struct. (Theochem)*, 395/396 (1997) 225–244.
[23] J.L. Asensio, M. Martín-Pastor, J. Jiménez-Barbero, *J. Mol. Struct. (Theochem)*, 395/396 (1997) 245–270.
[24] C.L.O. Petkowicz, F. Reicher, K. Mazeau, *Carbohydr. Polymers*, 37 (1998) 25–39.
[25] C.A. Stortz, A.S. Cerezo, *J. Carbohydr. Chem.*, 13 (1994) 235–247.
[26] C.A. Stortz, A.S. Cerezo, *An. Asoc. Quim. Argent.*, 83 (1995) 171–181.
[27] C.A. Stortz, A.S. Cerezo, *J. Carbohydr. Chem.*, 17 (1998) 1405–1419.
[28] T. Kozár, F. Petrák, Z. Gálová, I. Tvaroška, *Carbohydr. Res.*, 204 (1990) 27–36.
[29] S.W. Homans, M. Forster, *Glycobiology*, 2 (1992) 143–151.
[30] K.-H. Ott, B. Meyer, *Carbohydr. Res.*, 281 (1996) 11–34.
[31] F. Guarnieri, W.C. Still, *J. Comput. Chem.*, 15 (1994) 1302–1310.
[32] A. Bernardi, L. Raimondi, D. Zanferrari, *J. Mol. Struct. (Theochem)*, 395/396 (1997) 361–373.
[33] N.L. Allinger, Y.H. Yuh, J-H. Lii, *J. Am. Chem. Soc.*, 111 (1989) 8551–8566.
[34] MM3 (96), *Bull. QCPE*, 17 (1997) 3.
[35] C.A. Stortz, *An. Asoc. Quim. Argent.*, 86 (1998) 94–103.
[36] R.U. Lemieux, K. Bock, T.J. Delbaere, S. Koto, V.S. Rao, *Can. J. Chem.*, 58 (1980) 631–653.
[37] K. Mazeau, S. Pérez, *Carbohydr. Res.*, 311 (1998) 203–217.
[38] J. O'M. Bockris, A.K.N. Reddy, *Modern Electrochemistry*, Plenum Publishing Co, New York, 1970.
[39] S. Homans, *Biochemistry*, 29 (1990) 9110–9118.
[40] J. Koca, *J. Mol. Struct. (Theochem)*, 308 (1994) 13–24.
[41] J. Koca, S. Pérez, A. Imberty, *J. Comput. Chem.*, 16 (1995) 296–310.
[42] B.J. Hardy, *J. Mol. Struct. (Theochem)*, 395/396 (1997) 187–200.
[43] K. Rasmussen, J. Fabricius, *ACS Symp. Ser.*, 430 (1990) 177–190.